

Long-Term Climatic Transitions and Stochastic Resonance

C. Nicolis¹

Stochastic resonance constitutes one of the few plausible mechanisms capable of explaining the recurrent climatic changes that occurred on earth during the Quaternary era. In this paper early attempts and more recent progress to model these phenomena on a global scale are reviewed.

KEY WORDS: Stochastic resonance; ice ages; chaos in geophysics.

1. INTRODUCTION

Stochastic resonance is increasingly becoming a concept of universal validity. One realizes that the issue of enhanced sensitivity to small external forcings may be instrumental for the understanding of phenomena of current and primary concern in quite different contexts. This is undoubtedly the reason why the NATO workshop on *stochastic resonance* has managed to bring together researchers from unusually different horizons, a fact that is well reflected by the wide range of disciplines represented in the present special issue of the *Journal of Statistical Physics*.

Despite the variety we have just pointed out, one nevertheless notices that in their vast majority the papers presented deal either with general-purpose mathematical models or with phenomena that belong to the traditional realm of physical science; in other words, phenomena that unfold on time and space scales easily accessible to laboratory experiment. In this paper we discuss stochastic resonance on the quite different and, to some extent, more impressive scale of phenomena related to global climate. Curiously, it so happens that this more exotic context is also the one on which stochastic resonance was first introduced in the scientific literature some 10 years ago.^(1, 2)

¹ Institut Royal Météorologique de Belgique, 1180 Bruxelles, Belgium.

According to all elements of information at our disposal, the climatic system possesses a very pronounced internal variability. A striking illustration of this property is given by the last glaciation. During its peak, about 18,000 years ago, in the Northern hemisphere the Laurentide ice sheet covered most of Canada, New England, and much of the Middle West, Great Plains, and Rockies, whereas the Fenno-Scandian ice sheet extended into Eastern and Central Europe. In the Southern hemisphere ice sheets developed also over parts of Australia and New Zealand and extended out of the Andes.⁽³⁾ During this period the mean temperature of the globe was a few degrees lower than it is today, whereas the total volume of ice trapped in glaciers was more than two times larger than its present value of $30 \times 10^6 \text{ km}^3$. After these extreme conditions and in a time span of the order of a few thousand years the ice retreated to essentially the areas that it occupies today: Antarctica, Greenland, the Canadian Archipelago, and small mountain glaciers. In other words, the planet earth, a physical system, has in a few thousand years (a short time on a geological scale) undergone a transition between two extraordinary different states whose difference extends over the dimensions of the earth itself!

Going further back in the past, one now realizes that glaciations have actually covered, in an intermittent fashion, much of the Quaternary era. Figure 1 depicts the variation of the continental ice volume on earth over the last 10^6 years associated with these glacial-interglacial transitions as inferred from the oxygen isotope record of deep sea cores.⁽⁴⁾ Statistical data analysis shows that these major climatic episodes present an average periodicity of about 10^5 years to which is superimposed a considerable, random-looking variability (Fig. 2). This is intriguing, since the only known time scale in the range of 10^5 years refers to the change of eccentricity of

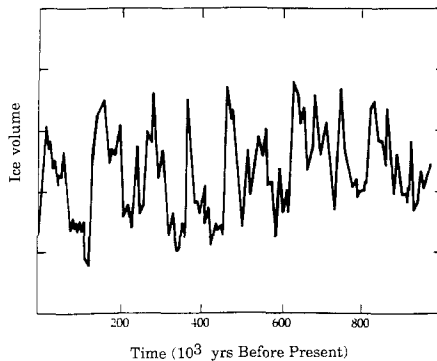


Fig. 1. Total volume of ice on earth during the last million years as deduced from deep sea core V28-238.⁽⁴⁾

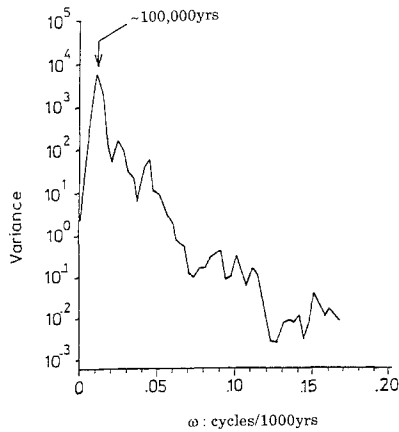


Fig. 2. Typical variance spectrum of climatic variability over the last million years.

the earth's orbit in time as a result of the perturbing action of the other bodies of the solar system. This perturbation in turn modifies the total solar energy received by the earth. Now the magnitude of this astronomical effect turns out to be exceedingly small, about 0.1%.⁽⁵⁾ The question therefore naturally arises, whether one can identify in the global dynamics of the earth-atmosphere-cryosphere system mechanisms capable of enhancing the sensitivity of the system to such small external periodic forcings. This was, precisely, the motivation of the early work on stochastic resonance.

Our principal objective in this paper is first, to summarize these early attempts, and subsequently, to comment on more recent developments in this particular field aiming to understand the sensitivity properties of the global climate. More specifically, in Section 2 a simple energy-balance-based model of glaciation cycles, viewed as a fluctuation-induced transition between multiple states enhanced by stochastic resonance, is analyzed. In Section 3 the possibility that glaciation cycles arise from internally generated oscillations or chaos is explored on the basis of coupled energy and mass balance equations. The main conclusions are drawn in Section 4.

2. STOCHASTIC RESONANCE AND GLACIATION CYCLES

Let us argue in very global terms, considering the earth as a zero-dimensional object in space receiving solar radiation and emitting in turn infrared radiation back to space. In such a view the relevant state variable

is the mean annual global average temperature T , which evolves in time according to the energy balance equation

$$\begin{aligned} C \frac{dT}{dt} &= \text{Incoming radiation} - \text{Outgoing radiation} + \text{Statistical fluctuations} \\ &= Q[1 - a(T)] - \varepsilon_B \sigma T^4 + F(t) \end{aligned} \quad (1)$$

Here C is the heat capacity; Q the solar constant; a the albedo, expressing the part of solar radiation reflected back to space [the temperature dependence anticipated in Eq. (1) accounts for the surface–albedo feedback]; σ the Stefan constant; and ε_B an emissivity factor accounting for deviations from the blackbody radiation law. For simplicity the random force term $F(t)$ is modeled as a Gaussian white noise

$$\langle F(t) \rangle = 0, \quad \langle F(t) F(t') \rangle = q^2 \delta(t - t') \quad (2)$$

Satellite data suggest that for temperature values T near the present-day climate, $a(T)$ is roughly a linear function of its argument. On the other hand, for very low T , $a(T)$ must tend to the albedo of ice, a_{ice} , whereas for high T , $a(T)$ should also saturate to some value a_{hot} descriptive of an ice-free earth. The simplest representation taking these features into account is the following piecewise linear model⁽⁶⁾:

$$\begin{aligned} 1 - a(T) &= 1 - a_{\text{ice}} & T < T_1 \\ 1 - a(T) &= 1 - (\alpha - \beta T) & T_1 < T < T_2 \\ 1 - a(T) &= 1 - a_{\text{hot}} & T > T_2 \end{aligned} \quad (3)$$

Furthermore, in view of the orbital variations alluded to in the Introduction, we decompose Q into an unperturbed part Q_0 and a periodic forcing,

$$Q = Q_0(1 + \varepsilon \sin \omega t) \quad (4)$$

where $\varepsilon \approx 0.001$ and $\omega = 2\pi/10^5 \text{ yr}^{-1}$.

Now the crucial point, illustrated in Fig. 3, is to realize that for plausible parameter values and in the absence of both stochastic and periodic forcings ($q=0$, $\varepsilon=0$) the energy budget predicts, typically, two stable climates. One of them, T_+ , corresponds to present-day conditions, whereas the other one, T_- , corresponds to a very low temperature and may be taken to represent a glaciation climate. These stable climates are separated by an intermediate unstable one, T_0 . As a result, Eq. (1) provides a typical illustration of the by now *classical setting of stochastic resonance*.

In the work reported earlier⁽¹⁾ we considered the case of “coexistence” of the two stable states T_+ and T_- in the sense that the probability

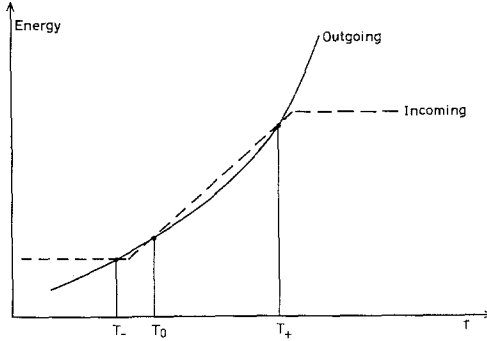


Fig. 3. Incoming and outgoing radiative energy as function of the global average temperature T . Their intersections at T_+ , T_- , and T_0 are the three steady states of Eq. (1) with $\varepsilon=0$, $q^2=0$. Parameter values: $Q = 340 \text{ W m}^{-2}$, $a_{\text{ice}} = 0.82$, $a_{\text{hot}} = 0.25$, $\beta = 0.0075$, and $\varepsilon_B = 0.61$.

masses in the two attraction basins of Eq. (1) with $\varepsilon=0$ are of the same order of magnitude. Recently⁽⁷⁾ evidence has been produced that this situation is in complete agreement with the statistical analysis of the record (Fig. 1).

The analysis was based on the Fokker–Planck equation corresponding to (1). This equation was first reduced, using the adiabatic approximation, to a closed equation for the total probability mass in one of the attraction basins⁽⁸⁾ (say the left one)

$$\dot{N}_- = r_+(t) - [r_-(t) + r_+(t)]N_- \quad (5)$$

where

$$r_{\pm} = \frac{1}{2\pi} |U''(T_0, t) U''(T_{\pm}, t)|^{1/2} \exp \left[-\frac{2}{q^2} \Delta U_{\pm}(t) \right] \quad (6)$$

$$\Delta U_{\pm}(t) = U(T_0, t) - U(T_{\pm}, t)$$

and the kinetic potential $U(T, t)$ is given by

$$U(T, t) = - \int^T dT' \{ Q_0(1 + \varepsilon \sin \omega t)[1 - a(T')] - \varepsilon_B \sigma T'^4 \} \quad (7)$$

To solve Eq. (5), we set

$$N_-(t) = N_0 + \varepsilon \hat{N}_- \sin(\omega t + \varphi) \quad (8)$$

where N_0 is the stationary solution of Eq. (5) in the absence of the forcing ($N_0 \sim 0.5$). Expanding Eqs. (5)–(7) in ε and keeping only linear terms, one

finds that the amplitude of the response \hat{N}_- depends crucially on the ratio of the two characteristic times of the problem: that is, the Kramers time τ_{Kr} and the periodicity of the forcing ω^{-1} :

$$\hat{N}_- \sim \frac{2}{q^2} [1 + (\tau_{Kr}\omega)^2]^{-1/2} \quad (9)$$

For physical values of q^2 and ΔU_{\pm} , τ_{Kr} is very large. Therefore, if ω is of the order of 1, the inverse square root factor would be exceedingly small and the response to this type of forcing would be negligible.

The situation is completely different if ω^{-1} is of the same order of magnitude as (or less than) τ_{Kr} . With the value of q^2 for which this equality is achieved one finds an amplification of the response of $\sim 20\%$, which is quite appreciable, considering the smallness of the amplitude of the periodic forcing ε . Similar conclusions have been reached independently and almost simultaneously by Benzi and co-workers⁽²⁾ on the basis of computer simulations of the Langevin equation (1).

Furthermore, from the perturbative solution of (5) the phase shift between the forcing and the response is found to be

$$\varphi = -\text{arctg}(\tau_{Kr}\omega) \quad (10)$$

The Fokker-Planck equation associated to (1) was also integrated numerically using a method developed by Chang and Cooper.⁽⁹⁾ Curve (a) of Fig. 4 depicts the time variation of the probability mass in the low-

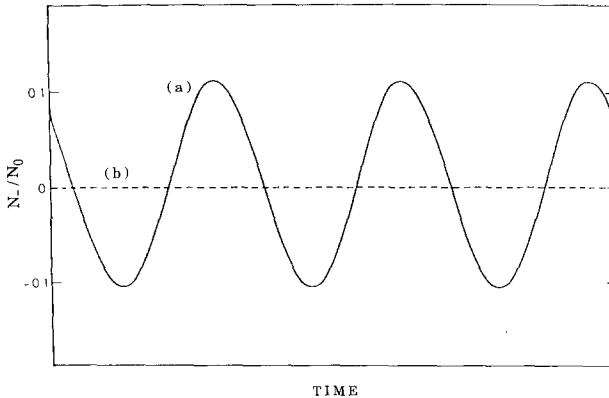


Fig. 4. Time evolution during 3 cycles of the probability mass in the low-temperature attraction basin N_- , normalized by its steady-state value N_0 , in the presence of a periodic forcing with $\varepsilon=0.001$ and (a) $\omega=2\pi/10^5 \text{ yr}^{-1}$, simulating the variation of the eccentricity of the earth's orbit, and (b) $\omega=2\pi/11 \text{ yr}^{-1}$, simulating a possible variation of the solar constant with the sunspot cycle. Time scale is normalized in such a way that $C=1$ in Eq. (1).

temperature attraction basin N_- normalized by its value in the absence of the forcing, N_0 . Choosing the variance of fluctuations q^2 such that $\omega \sim \tau_{Kr}^{-1}$, we observe, in accordance with the analytical results, an amplification of the probability mass of the order of 20%. There is a considerable time lag between forcing and response: As it turns out the maximum of the response lags behind the forcing by about 45° (12,500 years), in quantitative agreement with Eq. (10). For comparison we show in curve (b) the response to an 11-year solar cycle simulating a possible variation of the solar influx with the sunspot cycle. We see that the variation is now practically negligible.

The dramatic amplification of the response to an external periodic forcing in the presence of fluctuations has been referred to as *stochastic resonance*. As one sees from the analysis, this phenomenon is not to be confused with resonance in the usual sense of the term. It constitutes a new mechanism of amplification relying explicitly on the presence of both periodic and stochastic forcings.

3. SELF-GENERATED OSCILLATORY BEHAVIOR AND GLACIATION CYCLES

The intermittent character of the Quaternary glaciations and, more generally, of long-term climatic changes suggests the alternative scenario whereby the earth-atmosphere-cryosphere system would produce aperiodic self-sustained oscillations. Potentially, such a behavior may arise from the interaction between surface energy balance and mass balance of the cryosphere. A typical model describing the coupling between these processes is the one proposed by Saltzman and co-workers.⁽¹⁰⁾ In dimensionless excess variables it reads

$$\begin{aligned} \frac{d\eta}{dt} &= \theta - \eta \\ \frac{d\theta}{dt} &= b\theta - a\eta - \eta^2\theta \end{aligned} \tag{11}$$

where a, b are positive parameters and η, θ stand, respectively, for the sea-ice extent and mean ocean surface temperature. Equations (11) predict two types of behavior:

(i) $a > b$. For $b \geq 1$ a stable limit cycle bifurcates from the steady state. For reasonable parameter values inferred from the time scales of the processes present its period is of the order of a few thousand years. This is quite far from the dominant 10^5 -year scale suggested from the record in Fig. 2. Even if the periods could be matched, the oscillatory behavior

predicted would be incompatible with the random-looking character of the data (Fig. 1). One might of course enlarge Eqs. (11) by stochastic and periodic forcings modeling, respectively, the variation of the earth's orbit and the complexity of the environment.⁽¹¹⁾ However, these refinements would again produce behaviors very different from the record, which is reminiscent of transitions between two preferred states rather than of a noisy periodicity.⁽⁷⁾ This scenario is, therefore, to be dismissed.

(ii) $b > a$. In this range Eqs. (11) give rise to a phase portrait reminiscent of the dissipative Duffing oscillator.⁽¹²⁾ One can show that for reasonable parameter values this oscillator can be brought close to a homoclinic bifurcation. Under the action of a weak periodic forcing simulating orbital variations, such a system shows, once again, a pronounced sensitivity. Specifically, a qualitative change of regime can take place, leading to a chaotic attractor.

More technically, introducing the new variable

$$\xi = \theta - \eta \quad (12)$$

and the parameters

$$\begin{aligned} \varepsilon_1 &= b - 1 \\ \varepsilon_2 &= b - a \end{aligned} \quad (13)$$

one can write the augmented form of Eqs. (11) including the periodic forcing as

$$\begin{aligned} \frac{d\eta}{dt} &= \xi \\ \frac{d\xi}{dt} &= \varepsilon_1 \xi + \varepsilon_2 \eta - \eta^3 - \eta^2 \xi + s \sin \omega t \end{aligned} \quad (14)$$

where s and ω are, respectively, the amplitude and frequency of the forcing. Performing the following scaling of variables and parameters,

$$\begin{aligned} \eta &= x\mu, & \xi &= y\mu^2, & s &= p\mu^4 \\ \varepsilon_1 &= \gamma_1\mu^2, & \varepsilon_2 &= \gamma_2\mu^2, & \mu &\ll 1 \\ t &= \tau\mu^{-1}, & \omega &= \Omega\mu \end{aligned} \quad (15)$$

one may further write (14) as

$$\begin{aligned} \frac{dx}{d\tau} &= y \\ \frac{dy}{d\tau} &= \gamma_2 x - x^3 + \mu(\gamma_1 y - x^2 y + p \sin \Omega\tau) \end{aligned} \quad (16)$$

These equations can be viewed as the perturbations (for $\mu \ll 1$) of a reference system described by

$$\begin{aligned}\frac{dx_0}{d\tau} &= y_0 \\ \frac{dy_0}{d\tau} &= \gamma_2 x_0 - x_0^3\end{aligned}\tag{17}$$

This is a Hamiltonian system corresponding to the conservative Duffing oscillator.⁽¹²⁾ It exhibits a continuum of periodic trajectories as well as a pair of homoclinic orbits existing for all positive values of the parameter γ_2 . Going from Eqs. (17) to Eqs. (16) amounts therefore to inquiring how this phase space structure and, in particular, the infinite-period homoclinic orbits are perturbed by both the “dissipative” terms $\gamma_1 y - x^2 y$ and by the periodic forcing.

This problem can be formulated analytically. Setting $x = x_0 + \mu u$, $y = y_0 + \mu v$, we obtain the following equations for the perturbations u , v :

$$\begin{aligned}\frac{du}{d\tau} &= v \\ \frac{dv}{d\tau} &= (\gamma_2 - 3x_0^2)u + \gamma_1 y_0 - x_0^2 y_0 + p \sin \Omega\tau\end{aligned}\tag{18}$$

This is an inhomogeneous system of equations, which admits a nonsingular solution provided that a solvability condition is satisfied. The latter is given by the *Melnikov integral*⁽¹³⁾:

$$\int_{-\infty}^{\infty} d\tau y_0 (\gamma_1 y_0 - x_0^2 y_0 + p \sin \Omega\tau) = 0\tag{19}$$

This relation allows us to identify a critical forcing amplitude p_c beyond which the homoclinic orbit is destroyed by the periodic perturbation. One obtains, after a lengthy calculation,⁽¹⁴⁾

$$p_c = \frac{1}{3} \gamma_2^{3/2} \left(\gamma_1 - \frac{4}{5} \gamma_2 \right) \frac{\text{ch}[\Omega\pi/(2\gamma_2)^{1/2}] + 1}{\text{ch}[\Omega\pi/2(2\gamma_2)^{1/2}]}\tag{20}$$

In the theory of dynamical systems one shows that for $p > p_c$ a variety of complex nonperiodic behaviors may arise.⁽¹⁵⁾ Figure 5 depicts a typical time series obtained from numerical simulation in this region, along with the corresponding power spectrum. One obtains an aperiodic behavior in the form of intermittent transitions between two phase space regions. It is

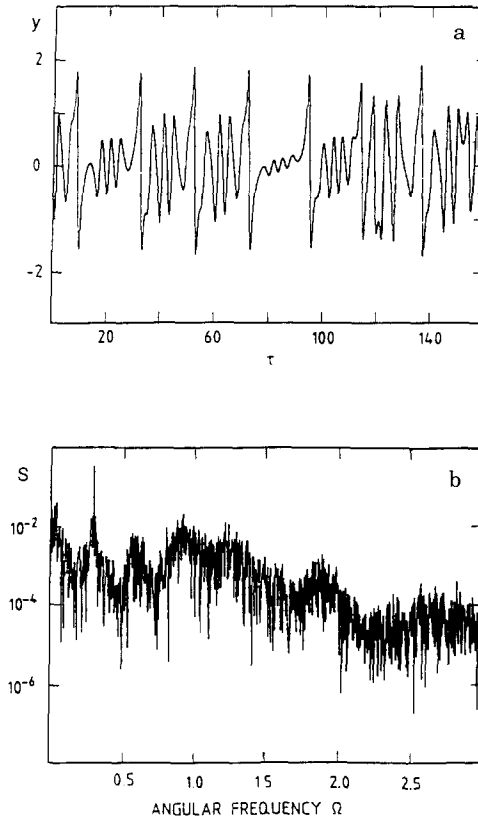


Fig. 5. Time evolution of (a) the variable y and (b) power spectrum of variable x for system (16) in the parameter region for which it admits aperiodic behavior. Parameter values: $\gamma_1 = 1.01$, $\gamma_2 = 1$, $\mu = 0.1$, $\Omega = 0.3$, and $p = 50p_c$ ($p_c = 0.148$). This latter value corresponds to a forcing amplitude of the initial equations (14) of $s \sim 7 \times 10^{-4}$.

noteworthy that the power spectrum exhibits an important broad-band component, a dominant, sharp peak at the forcing frequency, and a less pronounced and more noisy peak close to the unforced system's self-oscillation frequency (equal to about 3 times the forcing frequency). The similarity with paleoclimatic spectra (Fig. 2) is rather striking, considering the simplicity of the model. It suggests that deterministic chaos provides a plausible scenario of Quaternary climatic changes. This view is further corroborated by a dynamical reconstruction starting from the time series data of Fig. 1, which suggests the existence of a low-dimensional (between 3 and 4) chaotic attractor governing the dynamics in this time scale.⁽¹⁶⁾

4. CONCLUDING REMARKS

We have identified a mechanism of climatic variability based on stochastic resonance, enabling the earth-atmosphere-cryosphere system to respond sensitively to small-amplitude external periodic forcings arising from the variability of the earth's orbit. Furthermore, we have pointed out that the aperiodic character of climatic variability could also be associated with internally generated deterministic chaos.

Far from being contradictory, these two scenarios of long-term climatic change present interesting complementarities. Specifically, the picture of a bistable system performing fluctuation-driven intermittent jumps between two states can be viewed as a short-hand description of a chaotic attractor (see also the paper by Nicolis *et al.* in this issue⁽¹⁷⁾). In this view, the deterministic part and the random force in Eq. (1) represent, respectively, the large-scale structure of the underlying chaotic attractor and the "effective" noise that is intrinsically generated by the dynamics.⁽¹⁸⁾ Naturally, a more satisfactory approach would be to model such a noise as a highly correlated process rather than as a white noise one. As shown in other contributions in this issue, the theory of stochastic resonance can be amended to take this refinement into account without any substantial change in the overall philosophy.

ACKNOWLEDGMENTS

This work is supported, in part, by the Commission of the European Communities under contract SC1*-CT91-0697 (TSTS).

REFERENCES

1. C. Nicolis, *Solar Phys.* **74**:473 (1981); C. Nicolis, *Tellus* **34**:1 (1982).
2. R. Benzi, A. Sutera, and A. Vulpiani, *J. Phys. A* **14**:L453 (1981); R. Benzi, G. Parisi, A. Sutera, and A. Vulpiani, *Tellus* **34**:10 (1982).
3. H. H. Lamb, *Climate: Present, Past and Future*, Vol. 2 (Methuen, London, 1977).
4. N. J. Shackleton and N. D. Opdyke, *Quat. Res.* **3**:39 (1973).
5. A. L. Berger, *Quat. Res.* **9**:139 (1978).
6. C. Crafoord and E. Källén, *J. Atmos. Sci.* **35**:1123 (1978).
7. G. Matteucci, *Climate Dynamics* **5**:35 (1990).
8. C. Gardiner, *Handbook of Stochastic Methods* (Springer, Berlin, 1983).
9. J. S. Chang and G. Cooper, *J. Computational Phys.* **6**:1 (1970).
10. B. Saltzman, A. Sutera, and A. R. Hansen, *J. Atmos. Sci.* **39**:2634 (1982).
11. C. Nicolis, *Tellus* **36A**:217 (1984).
12. J. Guckenheimer and P. Holmes, *Nonlinear Oscillations, Dynamical Systems and Bifurcations of Vector Fields* (Springer-Verlag, Berlin, 1983).

13. V. K. Melnikov, *Trans. Moscow Math. Soc.* **12**(1):1 (1963).
14. C. Nicolis, *Tellus* **39A**:1 (1987).
15. C. Baesens and G. Nicolis, *Z. Phys. B. Condensed Matter* **52**:345 (1983).
16. C. Nicolis and G. Nicolis, *Nature* **311**:529 (1984).
17. G. Nicolis, C. Nicolis, and D. McKernan, *J. Stat. Phys.* **70**:125 (1993).
18. C. Nicolis and G. Nicolis, *Phys. Rev. A* **34**:2384 (1986).